RSC Advances

PAPER

View Article Online
View Journal | View Issue

Cite this: *RSC Adv.*, 2020, **10**, 29618

Synthesis, characterization, and catalytic application of hierarchical nano-ZSM-5 zeolite

Yanming Jia, *[a] Qinghua Shi,[a] Junwen Wang,[b] Chuanmin Ding[b] and Kan Zhang[c]

Hierarchical nano-ZSM-5 zeolites (Z5-*X*) with different grain sizes were synthesized by varying amounts of 3-glycidoxypropyltrimethoxysilane (KH-560) in the hydrothermal synthesis strategy. Moreover, the conventional ZSM-5zeolite(Z5), which was prepared without KH-560, was used as the reference sample. The crystalline phases, morphologies, porous characteristics, Si/Al molar ratios and acidic properties of all fresh catalysts were characterized using the X-ray diffraction (XRD), Fourier transform infrared spectra (FT-IR), scanning electron microscopy (SEM), N_2 adsorption–desorption, inductively coupled plasma atomic emission spectroscopy (ICP) and temperature programmed desorption of ammonia (NH_3-TPD) techniques. Results show that the grain size and strong acid amount of zeolite decreased with the increasing amount of KH-560. The micropore surface areas and the corresponding volume of Z5-*X* changed less compared with Z5. Consequently, the high shape-selectivity of zeolite was preserved well under the addition of KH-560. However, the mesopore surface areas and the corresponding volume increased significantly with the increasing amount of KH-560. Benefiting from the abundant hierarchical structure, the Z5-*X* catalysts exhibited a larger coke capacity than the Z5 catalyst. The coke depositions of all the deactivated catalysts were characterized by the thermogravimetric technique (TG), and the results are indicative of the decreased average rate of coke deposition with an increasing amount of KH-560, which could result from the gradually reduced strong acid amount and the nano-sized crystallites. The catalytic performance of methanol-to-aromatics (MTA) indicates that the Z5-0.12 catalyst exhibited higher catalytic activity and selectivity of BTX as the reaction was prolonged, which could result from the synergistic effect among the proper strong acid amount, the smaller zeolite grain size, and the abundant hierarchical structure.

Received 10th July 2020
Accepted 4th August 2020

DOI: 10.1039/d0ra06040b

rsc.li/rsc-advances

1. Introduction

As a kind of crystalline aluminosilicate, zeolites are composed of SiO_4 and AlO_4 tetrahedra, which link to form abundant uniform channels and cavities.[1] Meanwhile, zeolites are receiving great commercial interest due to their unique pore dimensions that are similar to the dynamics diameter of high-value chemicals.[2] In other words, zeolites have some characteristics and properties that are near those of a molecular sieve, such as shape-selectivity.[3] In particular, researchers have given significant attention to ZSM-5 zeolites due to their excellent selective chemical conversion in industrial applications.[4,5] Based on their unique structural features, like three-dimensional structure, ZSM-5 zeolites always display high selectivity to light aromatics (*e.g.*, benzene, toluene, and xylene-BTX) during the methanol to hydrocarbons (MTH) reaction.[6–8] In particular, the MTH process is considered a special milestone in the research field of zeolites and heterogeneous catalysis processes.[8]

Conventional ZSM-5 zeolites have a large grain size of the micrometer or sub-micrometer level, which inevitably increases the residence time of macromolecular intermediates and products in the inter channel.[9–11] Thus, the narrow pores of such zeolites are prone to be blocked quickly because of the coke deposition, leading to the sharp deactivation of zeolite catalysts.

Thus, many methods, like the preparation of nano-sized ZSM-5 [12–15] as well as hierarchical ZSM-5,[16–18] have been applied for the promotion of the diffusion property to enhance the catalyst stability of ZSM-5 zeolites. As the hierarchical ZSM-5 zeolites are concerned, the micropores of such zeolites involve remarkable shape-selectivity for the target products. Furthermore, the mesopores are beneficial for the transfer of macromolecules, and the coke capability of such zeolites are improved significantly. Accordingly, the catalytic performance of hierarchical ZSM-5 is obviously enhanced due to the advantageous properties of microporous zeolites and mesoporous materials.

[a]*Department of Chemistry, Taiyuan Normal University, PO Box 030619, Jinzhong, China. E-mail: jiayanmingtynu@163.com*

[b]*College of Chemistry and Chemical Engineering, Taiyuan University of Technology, Taiyuan, 030024, China*

[c]*State Key Laboratory of Coal Conversion, Institute of Coal Chemistry, Chinese Academy of Sciences, Taiyuan, 030001, China*

For the nano-sized ZSM-5, a small grain size implies a shorter inner diffusion path, which could transfer the heavy macromolecular products within a short period. Thus, the pore blockage derived deactivation of the catalyst will decelerate, and the catalyst lifetime of such zeolites increases significantly.

In our previous communication,[19] organosilane named 3-glycidoxypropyltrimethoxysilane (KH-560) was applied to prepare a hierarchical nano-ZSM-5 zeolites in a hydrothermal synthesis system. The use of organosilane could effectively inhibit zeolite crystal growth by the bond-blocking function, thereby producing the nano-sized zeolite crystals. Meanwhile, the intercrystalline mesopores among these nano-sized crystals could greatly enhance the coke capability of such zeolites. Thus, the hierarchical nano-ZSM-5 zeolites combine the advantages of nano-sized zeolites and hierarchical zeolites, and are a potential alternative for practical utilization.

In this research, the effects of the contents of KH-560 on the physical and chemical characteristics of Z5 zeolites are studied and discussed. Moreover, all the as-prepared Z5 zeolites are used for methanol to aromatics (MTA) reaction, respectively. The relationship between the MTA catalytic performance and the catalyst characteristics is built.

2. Experimental

2.1. Materials

All of the materials used for zeolites preparation are analytical reagents (ARs). Among of them, sodium hydroxide (NaOH), sodium chloride (NaCl), aluminum nitrate ($Al(NO_3)_3 \cdot 9H_2O$), and nitric acid (HNO_3) were acquired from Sinopharm Chemical Reagent Co., Ltd, China. SD-mode silica sol (SD-Si) was acquired from Dalian Snow Chemical New Material Science and Technology Co., Ltd, China. 3-Glycidoxypropyltrimethoxysilane (KH-560) and 25 wt% tetrapropylammonium hydroxide (TPAOH) were bought from Aladdin. Pseudo boehmite was obtained from Zibo Baida Chemical Co., Ltd, China. Sesbania powder was acquired from Westernization instrument Technology Co., Ltd, China. Distilled water (H_2O) was homemade.

2.2. Preparation of catalyst

The homogeneous Si–Al sol of the hierarchical nano-ZSM-5 zeolite (Z5-*X*) was prepared through following three steps:

(1) 0.528 g of NaOH and 1.45 g of NaCl were dissolved in 24 ml of H_2O. Afterward, 1.2384 g of $Al(NO_3)_3 \cdot 9H_2O$ was gradually added into the above aqueous solution. The resultant mixture was electromagnetically stirred continuously for 1 h, and the resultant clear solution was marked A.

(2) Quantitative (0–4.5 ml) KH-560 was added dropwise to 10 ml of TPAOH solution. The resultant solution was electromagnetically stirred for 1 h, the resultant clear solution was marked B.

(3) B was added to A slowly, and the resultant mixture was first stirred for 0.5 h. Then, 22.5 ml of SD-Si was dropwise added and, the resultant mixture was continuously stirred for another 2 h to achieve a homogeneous Si–Al sol. In particular, the molar compositions of the Si–Al sol was $38SiO_2 : 1Al_2O_3 : 4Na_2O : 7.5$ TPAOH : (0–12)KH-560 : $800H_2O : 15Cl^-$.

Table 1 Addition amount of KH-560 (ml) and corresponding molar ratio of KH-560/Si

KH-560 aq (ml)	0.91	1.94	3.13	4.50
KH-560/Si	0.06	0.12	0.18	0.24

In the end, the homogeneous sol was diverted to an autoclave, which was preheated for 12 h at 100 °C and then heated for another 72 h at 170 °C. The generated white solid was filtered and washed with distilled H_2O, then dried for 12 h at 100 °C and calcined for 5 h at 550 °C.

In order to obtain the acidic zeolites, the calcined solid was ion-exchange twice with 1 mol L^{-1} of NH_4NO_3 solution at 80 °C for 4 h each time. Subsequently, the resultant solid was dried for 12 h at 100 °C and calcined for 5 h at 550 °C. The resulting solid powder was denoted as Z5-*X*, where *X* refers to the molar ratio of KH-560/Si, and $X = 0.06, 0.12, 0.18, 0.24$ as is shown in Table 1.

The conventional ZSM-5 zeolites were similarly prepared without KH-560, and denoted as Z5. For obtain the extruded catalyst, four prepared zeolites powder were mixed respectively with pseudo boehmite, and the mass ratio of which was 4 : 1. Then, quantitative Sesbania powder was slowly added under constant stirring. After mixing completely, quantitative dilute HNO_3 (3%) was dropwise added, the mixture was squeezed to obtain a blocky catalyst. Finally, the blocky catalyst was extruded to strips, which were further dried for 12 h at 100 °C and calcined for 5 hat 550 °C.

2.3. Catalyst characterization

The crystalline information of the zeolites was investigated through power X-ray diffraction (XRD, SHIMADZU-6000) with the Cu Kα and scanning rate of 8° per min. Fourier transform infrared spectra were recorded in a FT-IR spectrometer (FT-IR, BRUKER TENSOR-27) with a resolution of 4 cm^{-1} using the KBr pellet technique. The surface area and the porous characteristics were analyzed using the N_2 adsorption–desorption analyzer (N_2 adsorption–desorption, BELSORP-max), the zeolites were degassed under 400 °C for 8 h before the measurement. The Si/Al molar ratios of the catalysts were determined by inductively coupled plasma atomic emission spectroscopy (ICP-AES, Autoscan16, TJA). The morphologies of the samples were observed using scanning electron microscopy (SEM, JSM 7001-F, JEOL). Moreover, the corresponding crystal size distribution were analyzed and counted by the software of Nano Measurer. Temperature programmed desorption of ammonia was performed through a chemisorption analyzer (NH_3-TPD, AutoChem II 2920). The specific testing process is as follows. At the Ar flow of 40 ml min^{-1}, the approximately 100 mg sample was heated to 300 °C at 10 °C min^{-1} for 2 h to remove adsorbed water. Then, the Ar was switched with NH_3 for 20 min after cooling down to 100 °C. Finally, the sample was heated to 700 °C at 10 °C min^{-1}, and the desorption NH_3 signal was

collected with a TCD detector. The thermogravimetric analysis was performed through a thermal analyzer (TG, Mettler TGA/SDTA851) within the temperature range of 50 °C to 700 °C at 10 °C min^{-1}.

2.4. Catalytic test

Before the measurement, the strip catalysts were crushed, and further sieved through a no. 20–40 sieve. 11 g of sieved catalyst were then placed in fixed-bed reactor for methanol conversion. In particular, the reactive tube is 90 cm in length and 16 mm in inner diameter, and the zeolite catalysts were loaded in the middle of the reactive tube filled with quartz pellets on both ends. Methanol was fed into the fixed-bed reactor through a double plunger pump. The reaction temperature, reaction pressure and the liquid weight hourly space velocity were 400 °C, 0.1 MPa and 1 h^{-1}, respectively. The gaseous products and liquid hydrocarbons were analyzed using GC-920 gas chromatography and GC-950 gas chromatography, respectively.

3. Results and discussion

3.1. Catalyst characterization

Fig. 1 displays the XRD spectra of the five prepared ZSM-5 catalysts. As we can see, the Z5, Z5-0.06, Z5-0.12 and Z5-0.18 catalysts displayed similar characteristic diffraction peaks in 2θ ranges of 8–10° and 22–25°, which are in alignment to the typical MFI crystal pattern.[20–22] However, the intensity and half width of the characteristic diffraction peaks are obviously different. Compared with the Z5 catalyst, the Z5-0.06, Z5-0.12 and Z5-0.18 catalysts displayed low and wide characteristic diffraction peaks, indicating that the nano-sized zeolite crystals were prepared.[17] Meanwhile, the intensity of the characteristic diffraction peaks gradually decreased with the increasing amount of KH-560. This may be largely ascribed to the gradually reduced grain size based on the Scherrer equation. In addition, a crystalline MFI zeolite is very difficult to obtain under a high amount of KH-560, and the Z5-0.24 catalyst is totally amorphous.

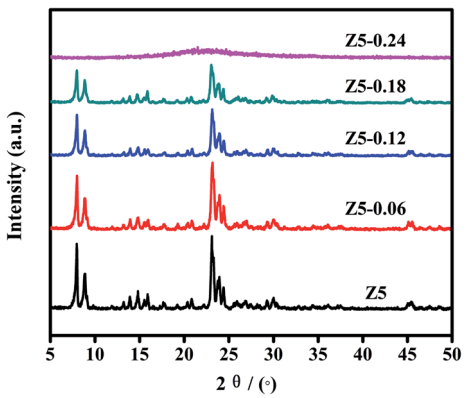

Fig. 1 XRD spectra of Z5, Z5-0.06, Z5-0.12, Z5-0.18 and Z5-0.24 catalysts.

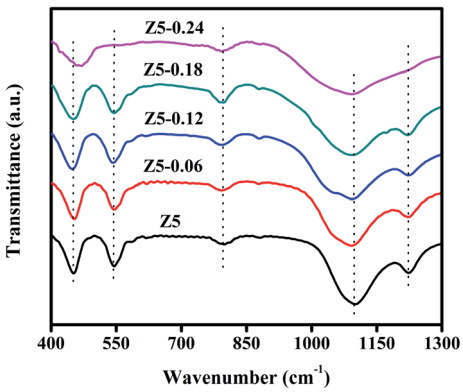

Fig. 2 FT-IR spectra of Z5, Z5-0.06, Z5-0.12, Z5-0.18 and Z5-0.24 catalysts.

Fig. 2 displays the FT-IR spectra of the five prepared ZSM-5 catalysts. As shown, the Z5, Z5-0.06, Z5-0.12 and Z5-0.18 catalysts show the FT-IR bands near 450, 547, 796, 1099 and 1222 cm^{-1}, which are characteristics of ZSM-5 framework.[23,24] Specially, the vibrational modes near 450, 796 and 1099 cm^{-1} are assigned to internal vibrations of SiO_4 or AlO_4 tetrahedra, which can also be observed in silica, quartz and cristobalite. However, the vibrational modes near 547 and 1222 cm^{-1} are assigned to the double-rings tetrahedra vibration and the asymmetric stretching of SiO_4 and AlO_4 tetrahedra in the zeolite framework, respectively.[25] For Z5-0.24 catalyst, no absorbance band at 547 and 1222 cm^{-1} could be observed, and the wavenumber near 450 cm^{-1} is ~20 cm^{-1} higher (blue shift) than that of Z5, Z5-0.06, Z5-0.12 and Z5-0.18 catalysts, these results further prove the amorphous nature of Z5-0.24 catalyst.

The morphologies of all the investigative ZSM-5 catalysts were observed by SEM techniques. As is shown in Fig. 3, all of the investigative ZSM-5 catalysts exhibit a spherical morphology, and the zeolite particle sizes of them are around 1.5 μm. However, their zeolite grain size is clearly different. As shown in Fig. 3A, the zeolite particles of Z5 catalyst are built by the accretion of abundant small crystallites. Moreover, the crystal size of Z5 catalyst are centered at 105–306 nm, and their average crystal diameter is around 193.9 nm as shown by the crystal size distribution. The average grain size of the Z5-0.06, Z5-0.12 and Z5-0.18 catalysts decreased with the addition of KH-560. Moreover, the average grain size gradually decreased with the increasing amount of KH-560. In particular, the zeolite particles of Z5-0.06 (Fig. 3B), Z5-0.12 (Fig. 3C) and Z5-0.18 (Fig. 3D) catalysts are built by the accretion of abundant nano-crystallites, and their average crystal diameters are approximately 61.5 nm, 53.7 nm and 24.5 nm, respectively. This result is well consistent with the XRD result. The accumulation of these nano-crystallites contributes to the formation of extensive intercrystal mesopores within these zeolite particles, which effectively increases the coke capacity of such zeolites.[19]

Fig. 4 displays the N_2 adsorption–desorption isotherms of the Z5, Z5-0.06, Z5-0.12 and Z5-0.18 catalysts. Similarly, all of the ZSM-5 catalysts show a high N_2 uptake at low relative pressure of $P/P_0 < 0.2$. Moreover, a hysteresis loop is observed at

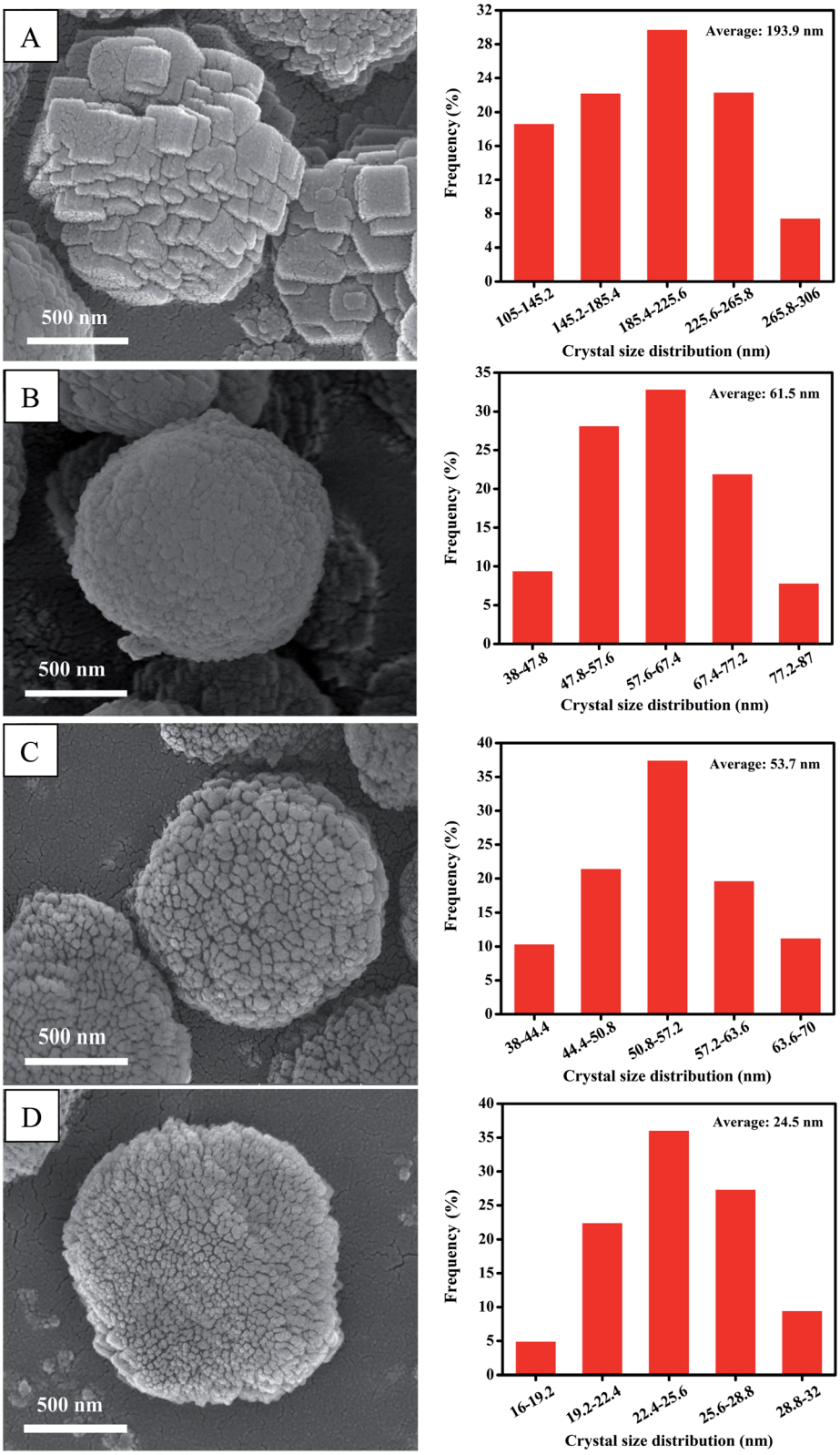

Fig. 3 SEM images (left) and corresponding crystal size distribution (right) of Z5 (A), Z5-0.06 (B), Z5-0.12 (C) and Z5-0.18 (D) catalysts.

high relative pressure of $P/P_0 > 0.4$, indicating that the intrinsic micropores and mesopores coexist in the four ZSM-5 catalysts. In particular, all of the ZSM-5 catalysts exhibit the IV-type isotherm with an H4-type hysteresis loop, which is generally observed in slit-like porous materials.[26] According to the SEM images (Fig. 3), we can reasonably come to the conclusion that

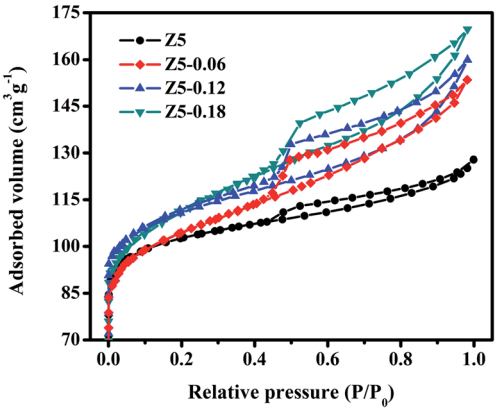

Fig. 4 N_2 adsorption–desorption isotherms of Z5, Z5-0.06, Z5-0.12 and Z5-0.18 catalysts.

the mesopores in the four ZSM-5 catalysts were built by the accretion of small crystallites or nanocrystals. It should be noted that a forced closure of hysteresis at a relative pressure of $P/P_0 = 0.42$ is observed in Z5-0.06, Z5-0.12 and Z5-0.18 catalysts, which could be due to the fact that the N_2 molecules in the mesopores are surrounded by the "micropore wall". Only when the specific release pressure of the molecule is reached, the N_2 molecules blocked in the mesoporous could be released rapidly. Specially, for further comparative investigation, the specific surface area and pore volume of the four ZSM-5 catalysts are calculated in Table 2.

As is shown in Table 2, the Z5-0.06, Z5-0.12 and Z5-0.18 catalysts exhibited higher BET surface areas (S_{BET}) with the addition of KH-560. Moreover, the BET surface areas increased with an increasing amount of KH-560. However, no trend in micropore surface areas (S_{micro}) could be determined, so no changes could be observed in relation to S_{BET} where an upward trend is indicated. Therefore, the increase in BET surface areas was caused by the increase in mesopore surface areas (S_{meso}). This analysis is well matched with the data shown in Table 2. Meanwhile, the trends of change of the total pore volume (V_{total}), the micropore volume (V_{micro}) and the mesopore volume (V_{meso}) is similar to those of S_{BET}, S_{micro}, and S_{meso}, respectively. All in all, the micropores intrinsically possessed by the ZSM-5 crystals changed lightly with the increasing amount of KH-560, thereby preserving the shape-selectivity of the ZSM-5 zeolite, while the mesopores generated by the accumulation of nanocrystals increased, which effectively increases the coke capacity of the ZSM-5 zeolites.

The Si/Al molar ratios of the four investigated ZSM-5 catalysts were determined by ICP analysis, and the results were also presented in Table 2. It is clear that the Si/Al ratio increases with the increasing amount of KH-560. We tentatively ascribe this to the increased Si content in synthetic gel.[27] Specifically, the KH-560 in synthetic gel could hydrolyze to produce the Si–OH, which were grafted on the MFI skeleton and acted as the Si source in the hydrothermal synthesis process, as a result, the ratio of Si/Al in the zeolite product increases.

The acidic properties of the Z5, Z5-0.06, Z5-0.12 and Z5-0.18 catalysts are measured by NH_3-TPD technique, and the corresponding NH_3 desorption profiles are shown in Fig. 5. According to the literature, the high temperature desorption peak above 350 °C is ascribed to the desorption of NH_3 from strongly acidic sites.[28,29] The low temperature desorption peak below 300 °C is due to the desorption of weakly bound NH_3. In particular, the weakly bound NH_3 is not the NH_3 adsorbed on weakly acidic sites, but possibly the hydrogen-bonded ammonia species.[30–32] The area of the NH_3 desorption peak can be used to measure the acid amount.[33,34] In order to achieve the strong acid amounts of the Z5, Z5-0.06, Z5-0.12 and Z5-0.18 catalysts, every NH_3-TPD profile was deconvoluted into three Gaussian peaks (green dashed lines), and the corresponding strong acid amounts were calculated in Table 3. Apparently, compared with the Z5 catalyst, the strong acid amount of the Z5-0.06, Z5-0.12 and Z5-0.18 catalysts decreased. Moreover, the strong acid amounts gradually decreased with the increasing amount of KH-560, which we tentatively ascribe to the increased Si/Al molar ratio as shown in Table 2.

3.2. MTA catalytic performance

All of the prepared ZSM-5 catalysts were used in the MTA reaction. Moreover, the MTA reaction was carried out at $T = 400$ °C, $P = 0.1$ MPa, WHSV = 1 h^{-1}. Fig. 6 shows the relationships between the methanol conversion and the time on-stream in the Z5, Z5-0.06, Z5-0.12 and Z5-0.18 catalysts. Clearly, the Z5 catalyst exhibited the poorest catalyst stability. However, the Z5-0.06, Z5-0.12 and Z5-0.18 catalysts showed improved catalyst stability with the addition of KH-560. We tentatively attribute this to the following two aspects. For one hand, the Z5-0.06, Z5-0.12 and Z5-0.18 catalysts have smaller nanometer scale, which effectively promoted the physical transport of macromolecular products in micropores, while the abundant inter-crystal mesopores in such zeolite particles largely increased the coke capacity of these catalyst.

Table 2 Textural properties of four investigated ZSM-5 catalysts

Sample	Al[a] (wt%)	Si[a] (wt%)	Si/Al[a]	S_{BET}[b] (m^2 g^{-1})	S_{micro}[c] (m^2 g^{-1})	S_{meso}[d] (m^2 g^{-1})	V_{total}[e] (cm^3 g^{-1})	V_{micro}[f] (cm^3 g^{-1})	V_{meso}[g] (cm^3 g^{-1})
Z5	2.25	43.17	18.50	353.6	261.3	92.3	0.214	0.102	0.112
Z5-0.06	2.09	43.35	20.00	390.4	263.9	126.5	0.236	0.102	0.134
Z5-0.12	2.03	43.60	20.71	418.0	276.1	141.9	0.249	0.105	0.144
Z5-0.18	1.95	44.18	21.85	429.0	268.5	160.5	0.256	0.103	0.153

[a] Determined by the ICP analysis. [b] Calculated by the BET method. [c] Calculated by the t-plot method. [d] $S_{meso} = S_{BET} - S_{micro}$. [e] Calculated from the adsorbed data at $P/P_0 = 0.995$. [f] Calculated by the *t*-plot method. [g] $V_{meso} = V_{total} - V_{micro}$.

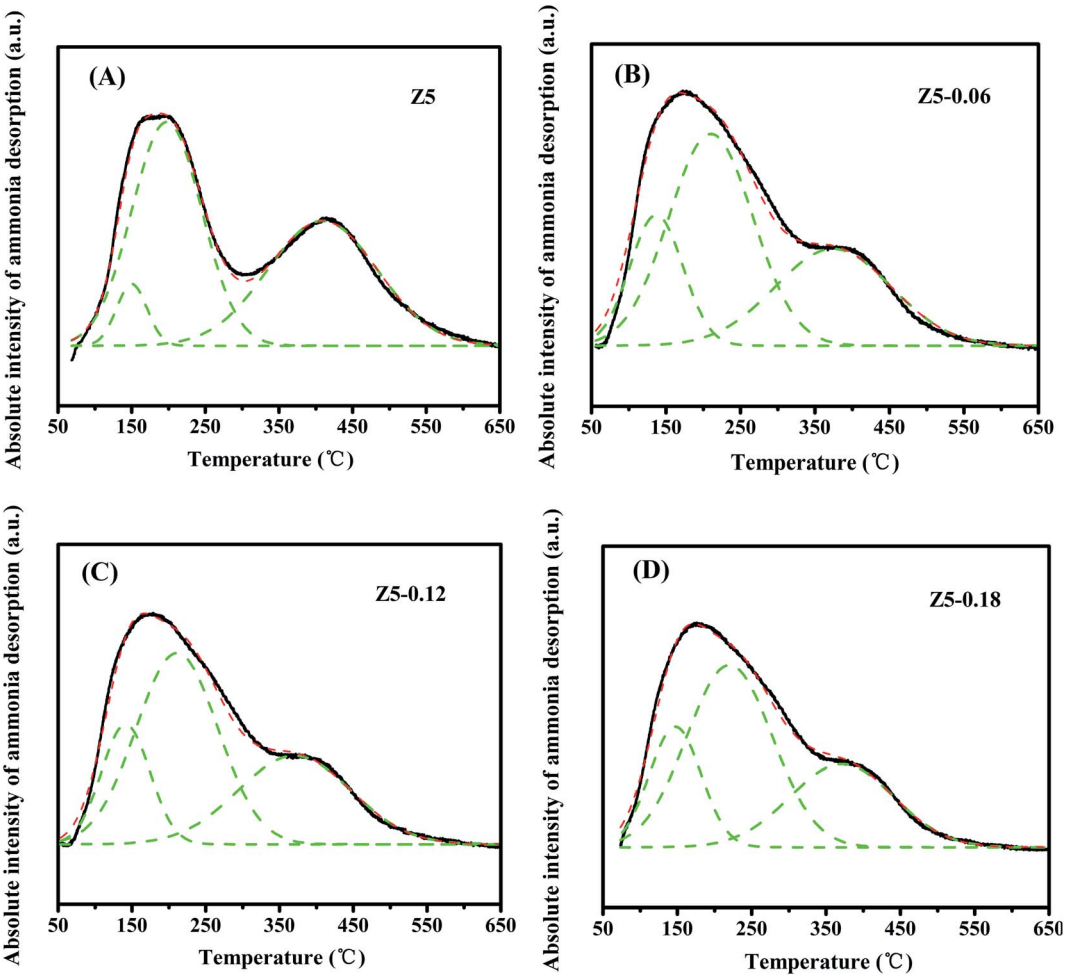

Fig. 5 NH_3-TPD profiles of Z5 (A), Z5-0.06 (B), Z5-0.12 (C) and Z5-0.18 (D). Green dashed lines show the Gaussian deconvolution peaks, red dashed lines show the cumulative fit peak.

Consequently, the catalyst deactivation result from the pore blocking decelerated, and the catalyst stability of such zeolites increased significantly. For another hand, compared with Z5 catalyst, the Z5-0.06, Z5-0.12 and Z5-0.18 catalysts have less strong acid amount, which effectively decelerated the severe coke deposition reaction to some extent. Thus the catalyst stability of such zeolites can be further improved.

In particular, the Z5 catalyst displayed a high catalytic activity in a short time on-stream of about 102 h. Subsequently, the methanol conversion quickly decreased to 40% at 138 h. Compared with Z5 catalyst, the Z5-0.06 catalyst has a high catalytic activity in a longer time on-stream, and the methanol conversion remained as high as >98% after 138 h, which is 58% higher than that of the Z5 catalyst. Moreover, the methanol conversion still remained more than 90% after 150 h. Similarly, the Z5-0.12 and Z5-0.18 catalysts showed a high catalytic activity

Table 3 Strong acid amounts of Z5, Z5-0.06, Z5-0.12 and Z5-0.18 catalysts calculated by NH_3-TPD profiles

Catalyst	Strong acid center (°C)	Strong acid amount (μmol g^{-1})
Z5	409	685.6
Z5-0.06	374	550.6
Z5-0.12	370	496.2
Z5-0.18	371	422.3

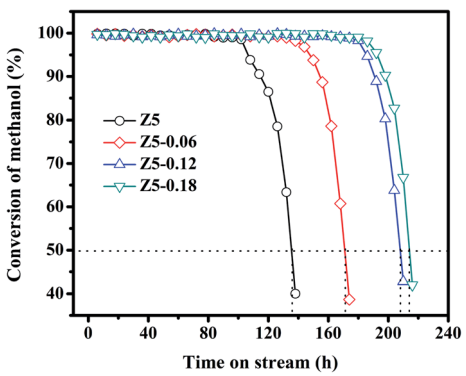

Fig. 6 Relationships between methanol conversion and time on-stream in the Z5, Z5-0.06, Z5-0.12 and Z5-0.18 catalysts.

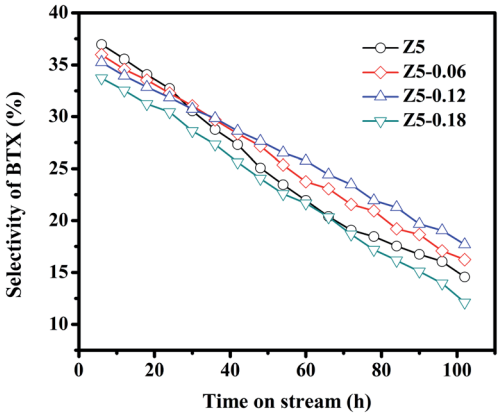

Fig. 7 Relationships between BTX selectivity and time on-stream in the Z5, Z5-0.06, Z5-0.12 and Z5-0.18 catalysts.

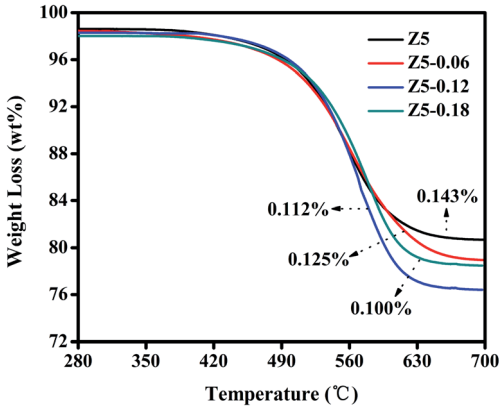

Fig. 8 TG curves of deactivated Z5, Z5-0.06, Z5-0.12 and Z5-0.18 catalysts.

within 180 h and 186 h of the reaction (>98%), respectively; subsequently, the methanol conversion dramatically decreased to less than 50% at 210 h and 216 h, respectively. According to the reports in the literature,[35] in the MTH reaction, the zeolite catalysts can be considered completely deactivated when the conversion of methanol is lower than 50%. Thus, the catalyst lifetimes of the Z5, Z5-0.06, Z5-0.12 and Z5-0.18 catalysts are around 135 h, 170 h, 208 hand 214 h, respectively.

The relationships between the BTX selectivity and the time on-stream in the Z5, Z5-0.06, Z5-0.12 and Z5-0.18 catalysts are shown in Fig. 7. Apparently, the selectivity of BTX in the four investigated ZSM-5 catalysts decreased as the reaction prolonged. This phenomenon may be largely attributed to the formation of coke species as the reaction prolonged. Specifically, the MTA reaction is a typical acid catalytic reaction,[36–38] in which numerous strongly acidic sites are conducive for generating BTX hydrocarbons. Nevertheless, the strongly acidic sites of catalysts are covered gradually by the coke species with the reaction process, and thus the BTX selectivity decreased gradually. Particularly, the Z5 catalyst displayed the highest BTX selectivity in the first 24 h of reaction, moreover, the initial BTX selectivity could reach as high as 36.95%, which we tentatively ascribe to its abundant strongly acidic sites as shown in the NH_3-TPD profiles (Fig. 5). After that, however, the Z5 catalysts exhibited lower selectivity of BTX than the Z5-0.06 and Z5-0.12 catalysts, and the selectivity of BTX falls to 14.58% after 102 h of reaction. This may be largely attributed to its higher average rate of coke deposition as shown in the TG profiles (Fig. 8). Therefore, a large number of coke species were deposited on the strongly acidic sites of the Z5 catalyst in a short time, and the BTX selectivity of such catalyst decreased significantly. Compared with Z5 catalyst, the Z5-0.06 and Z5-0.12 catalysts showed a lower BTX selectivity in the first 24 h of reaction. In particular, the initial selectivity of BTX of the two catalysts could respectively reach 35.97% and 35.25%, which is closely related to the less strongly acidic sites of the two catalysts. After that, however, the Z5-0.06 and Z5-0.12 catalysts exhibited a higher BTX selectivity, which respectively decreased to 16.24% and 17.68% after 102 h of reaction. This phenomenon is closely related to their lower average rate of coke deposition. The Z5-0.18 catalyst exhibited the lowest BTX selectivity during the entire reaction, and the initial BTX selectivity could reach 33.72%, which decreased to 12.12% after 102 h of reaction. This phenomenon may be largely attributed to its much fewer strongly acidic sites than Z5 catalyst.

The above results strongly indicate that the selectivity of BTX during the MTA reaction shows significant associations with the strong acid amount and the average rate of coke deposition. Moreover, the average rate of coke deposition shows significant associations with the strong acid amount and the diffusion characteristics of the catalyst. Therefore, the selectivity of BTX is closely related to the strong acid amount, grain size and hierarchical structure of the catalyst. A high selectivity of BTX could be obtained under the synergistic effect of a proper strong acid amount, smaller zeolite grain size, and abundant hierarchical structure.

In order to discuss the coke deposition on the deactivated ZSM-5 catalysts, we perform a thermogravimetric analysis. Moreover, the TG curves of the four deactivated catalysts after MTA reaction are shown in Fig. 8. As the figure shows, the TG curves of the four deactivated catalysts are quite similar. Nevertheless, the weight losses of these catalysts are clearly different. Specifically, the Z5 catalyst exhibited a low weight loss of around 19.32%, which is lower than that of the Z5-0.06 (21.26%), Z5-0.12 (23.27%), and Z5-0.18 (21.51%) catalysts. That is, the coke capacity of the ZSM-5 zeolite increased after KH-560 was added, which we tentatively ascribe to their increased mesopores formed by the buildup of the ZSM-5 nanocrystallites. Additionally, the weight loss per hour can be defined as the average coke deposition rate of the catalyst.[39] As shown in Fig. 6, the catalytic lifetimes of the Z5, Z5-0.06, Z5-0.12, and Z5-0.18 catalysts are approximately 135 h, 170 h, 208 h, and 214 h, respectively. Therefore, the average rates of coke deposition in the Z5, Z5-0.06, Z5-0.12, and Z5-0.18 catalysts are approximately 0.143%, 0.125%, 0.112%, and 0.100% per hour, respectively. Clearly, the average coke deposition rates decreased with an increasing amount of KH-560, which could

be reasonably ascribed to the synergistic effect between the reduced strong acid amount and the nano-sized crystallites.

4. Conclusions

Hierarchical nano-ZSM-5 zeolites (Z5-*X*) with different grain sizes were prepared by varying amounts of KH-560 in the hydrothermal synthesis strategy. The physicochemical properties, as well as the catalytic performance in MTA reaction for all of prepared catalysts were compared. The results show that the grain size of zeolite decreased with the increasing amount of KH-560, and thence the mesopores produced by the accumulation of nano-crystals increased, which was very beneficial to increasing the coke capacity of zeolites. Meanwhile, the changes in micropore volume and corresponding surface areas of Z5-*X* catalyst were not obvious compared with those of Z5 catalyst. Therefore, the shape-selectivity of the ZSM-5 zeolite was basically preserved. The strong acid sites decreased with the increasing amount of KH-560, which may largely be attributed to the increased Si/Al ratio. The average coke formation rate of zeolites decreased with the increasing amount of KH-560, which may be due to the synergistic effect between the gradually reduced strong acid amount and the nano-sized crystallites. The catalytic performance results indicate that Z5-0.12 catalyst exhibited higher selectivity of BTX and better catalytic activity as the reaction prolonged than the other catalysts, which is largely attributed to the synergistic effect among the proper strong acid amount, the smaller zeolite grain size, and the abundant hierarchical structure.

Conflicts of interest

There are no conflicts of interest to declare.

Acknowledgements

This work has been supported by the Scientific and Technological Innovation Programs of Higher Education Institutions in Shanxi (Grant No. 2019L0812); National Natural Science Foundation of China (Grant No. 21706178, 21978189); Natural Science Foundation of Shanxi Province (Grant No. 201801D221074, 201801D121058).

References

1 M. Boronat and A. Corma, What Is Measured When Measuring Acidity in Zeolites with Probe Molecules?, *ACS Catal.*, 2019, **9**, 1539–1548.
2 D. P. Serrano, J. Aguado, G. Morales, J. M. Rodríguez, A. Peral, M. Thommes, J. D. Epping and B. F. Chmelka, Molecular and Meso- and Macroscopic Properties of Hierarchical Nanocrystalline ZSM-5 Zeolite Prepared by Seed Silanization, *Chem. Mater.*, 2009, **21**, 641–654.
3 A. Corma, State of the art and future challenges of zeolites as catalysts, *J. Catal.*, 2003, **216**, 298–312.
4 Y. T. Cheng, Z. Wang, C. J. Gilbert, W. Fan and G. W. Huber, Production of p-xylene from Biomass by Catalytic Fast Pyrolysis Using ZSM-5 Catalysts with Reduced Pore Openings, *Angew. Chem., Int. Ed.*, 2012, **51**, 11097–11100.
5 A. Chawla, R. Li, R. Jain, R. J. Clark, J. G. Sutjianto, J. C. Palmer and J. D. Rimer, Cooperative effects of inorganic and organic structure-directing agents in ZSM-5 crystallization, *Mol. Syst. Des. Eng.*, 2018, **3**, 159–170.
6 A. A. Rownaghi and J. Hedlund, Methanol to Gasoline-Range Hydrocarbons: Influence of Nanocrystal Size and Mesoporosity on Catalytic Performance and Product Distribution of ZSM-5, *Ind. Eng. Chem. Res.*, 2011, **50**, 11872–11878.
7 X. J. Niu, J. Gao, K. Wang, Q. Miao, M. Dong, G. F. Wang, W. B. Fan, Z. F. Qin and J. G. Wang, Influence of crystal size on the catalytic performance of H-ZSM-5 and Zn/H-ZSM-5 in the conversion of methanol to aromatics, *Fuel Process. Technol.*, 2017, **157**, 99–107.
8 Y. M. Jia, J. W. Wang, K. Zhang, G. L. Chen, Y. F. Yang, S. B. Liu, C. M. Ding, Y. Y. Meng and P. Liu, Hierarchical ZSM-5 zeolite synthesized via dry gel conversion-steam assisted crystallization process and its application in aromatization of methanol, *Powder Technol.*, 2018, **328**, 415–429.
9 F. Rezaei and P. Webley, Structured adsorbents in gas separation processes, *Sep. Purif. Technol.*, 2010, **70**, 243–256.
10 K. Egeblad, C. H. Christensen, M. Kustova and C. H. Christensen, Templating Mesoporous Zeolites, *Chem. Mater.*, 2008, **20**, 946–960.
11 H. B. Zhang, Y. C. Ma, K. S. Song, Y. H. Zhang and Y. Tang, Nano-crystallite oriented self-assembled ZSM-5 zeolite and its LDPE cracking properties: Effects of accessibility and strength of acid sites, *J. Catal.*, 2013, **302**, 115–125.
12 M. Firoozi, M. Baghalha and M. Asadi, The effect of micro and nano particle sizes of H-ZSM-5 on the selectivity of MTP reaction, *Catal. Commun.*, 2009, **10**, 1582–1585.
13 M. Choi, K. Na, J. Kim, Y. Sakamoto, O. Terasaki and R. Ryoo, Stable Single-Unit-Cell Nanosheets of Zeolite MFI as Active and Long-Lived Catalysts, *Nature*, 2009, **462**, 246–249.
14 A. A. Rownaghi and J. Hedlund, Methanol to Gasoline-Range Hydrocarbons: Influence of Nanocrystal Size and Mesoporosity on Catalytic Performance and Product Distribution of ZSM-5, *Ind. Eng. Chem. Res.*, 2011, **50**, 11872–11878.
15 H. Konno, T. Tago, Y. Nakasaka, R. Ohnaka, J. Nishimura and T. Masuda, Effectiveness of nano-scale ZSM-5 zeolite and its deactivation mechanism on catalytic cracking of representative hydrocarbons of naphtha, *Micropor. Mesopor. Mater.*, 2013, **175**, 25–33.
16 J. J. Ding, H. Y. Liu, P. Yuan, G. Shi and X. J. Bao, Catalytic Properties of a Hierarchical Zeolite Synthesized from a Natural Aluminosilicate Mineral without the Use of a Secondary Mesoscale Template, *Chem. Cat. Chem.*, 2013, **5**, 2258–2269.
17 Z. Xue, J. Ma, J. Zheng, T. Zhang, Y. Kang and R. Li, Hierarchical structure and catalytic properties of a microspherical zeolite with intracrystalline mesopore, *Acta Mater.*, 2012, **60**, 5712–5722.

18 M. Moliner, C. Martinez and A. Corma, Multipore Zeolites: Synthesis and Catalytic Applications, *Angew. Chem., Int. Ed.*, 2015, **54**, 2–22.
19 Y. M. Jia, J. W. Wang, K. Zhang, W. Feng, S. B. Liu, C. M. Ding and P. Liu, Nanocrystallite self-assembled hierarchical ZSM-5 zeolite microsphere for methanol to aromatics, *Micropor. Mesopor. Mater.*, 2017, **247**, 103–115.
20 S. Wang, P. F. Wang, Z. F. Qin, Y. Y. Chen, M. Dong, J. F. Li, K. Zhang, P. Liu, J. G. Wang and W. B. Fan, Relation of Catalytic Performance to the Aluminum Siting of Acidic Zeolites in the Conversion of Methanol to Olefins, Viewed via a Comparison between ZSM-5 and ZSM-11, *ACS Catal.*, 2018, **8**, 5485–5505.
21 X. J. Niu, J. Gao, Q. Miao, M. Dong, G. F. Wang, W. B. Fan, Z. F. Qin and J. G. Wang, Influence of preparation method on the performance of Zn-containing HZSM-5 catalysts in methanol-to-aromatics, *Micropor. Mesopor. Mater.*, 2014, **197**, 252–261.
22 P. Wang, L. Chen, J. Xie, H. Li, C. T. Au and S. F. Yin, Enhanced catalytic performance in CH_3Br conversion to benzene, toluene, and xylene over steamed HZSM-5 zeolites, *Catal. Sci. Technol.*, 2017, **7**, 2559–2565.
23 P. Bai, P. P. Wu, W. Xing, D. L. Liu, L. M. Zhao, Y. H. Wang, B. J. Xu, Z. F. Yan and X. S. Zhao, Synthesis and catalytic properties of ZSM-5 zeolite with hierarchical pores prepared in the presence of n-hexyltrimethylammonium bromide, *J. Mater. Chem. A*, 2015, **3**, 18586–18597.
24 R. Sabarish and G. Unnikrishnan, Synthesis, characterization and catalytic activity of hierarchical ZSM-5 templated by carboxymethyl cellulose, *Powder Technol.*, 2017, **320**, 412–419.
25 T. Xue, Y. M. Wang and M. Y. He, Facile synthesis of nano-sized NH_4-ZSM-5 zeolites, *Micropor. Mesopor. Mater.*, 2012, **156**, 29–35.
26 A. A. Rownaghi, F. Rezaei and J. Hedlund, Uniform mesoporous ZSM-5 single crystals catalyst with high resistance to coke formation for methanol deoxygenation, *Micropor. Mesopor. Mater.*, 2012, **151**, 26–33.
27 P. Wang, L. Chen, J. K. Guo, S. Shen, C. T. Au and S. F. Yin, Synthesis of Submicron-Sized SAPO-34 as Efficient Catalyst for Olefin Generation from CH_3Br, *Ind. Eng. Chem. Res.*, 2019, **58**, 18582–18589.
28 Y. M. Ni, A. M. Sun, X. L. Wu, G. L. Hai, J. L. Hu, T. Li and G. X. Li, The preparation of nano-sized H[Zn, Al]ZSM-5 zeolite and its application in the aromatization of methanol, *Micropor. Mesopor. Mater.*, 2011, **143**, 435–442.
29 Y. Bi, Y. L. Wang, X. Chen, Z. X. Yu and L. Xu, Methanol aromatization over HZSM-5 catalysts modified with different zinc salts, *Chin. J. Catal.*, 2014, **35**, 1740–1751.
30 T. Miyamoto, N. Katada, J. H. Kim and M. Niwa, Acidic Property of MFI-Type Gallosilicate Determined by Temperature-Programmed Desorption of Ammonia, *J. Phys. Chem. B*, 1998, **102**, 6738–6745.
31 K. Nishi, S. Komai, K. Inagaki, A. Satsuma and T. Hattori, Structure and catalytic properties of Ga-MFI in propane aromatization, *Appl. Catal. A: General*, 2002, **223**, 187–193.
32 S. W. Choi, W. G. Kim, J. S. So, J. S. Moore, Y. J. Liu, R. S. Dixit, J. G. Pendergast, C. Sievers, D. S. Sholl, S. Nair and C. W. Jones, Propane dehydrogenation catalyzed by gallosilicate MFI zeolites with perturbed acidity, *J. Catal.*, 2017, **345**, 113–123.
33 M. Niwa, N. Katada, M. Sawa and Y. Murakami, Temperature-Programmed Desorption of Ammonia with Readsorption Based on the Derived Theoretical Equation, *J. Phys. Chem.*, 1995, **99**, 8812–8816.
34 X. X. Wang, J. F. Zhang, T. Zhang, H. Xiao, F. Song, Y. Z. Han and Y. S. Tan, Mesoporous ZnZSM-5 zeolites synthesized by one-step desilication and reassembly: A durable catalyst for methanol aromatization, *RSC Adv.*, 2016, **6**, 23428–23437.
35 T. V. W. Janssens, A new approach to the modeling of deactivation in the conversion of methanol on zeolite catalysts, *J. Catal.*, 2009, **264**, 130–137.
36 Y. Liu, Q. Q. Chang, M. Yang, E. Z. Liu and J. Fan, Research progress of methanol to aromatics, *Chem. Eng.*, 2015, **43**, 74–78.
37 H. Schulz, "Coking" of zeolites during methanol conversion: Basic reactions of the MTO-, MTP- and MTG processes, *Catal. Today*, 2010, **154**, 183–194.
38 R. Barthos, T. Bánsági, T. S. Zakar and F. Solymosi, Aromatization of methanol and methylation of benzene over Mo2C/ZSM-5 catalysts, *J. Catal.*, 2007, **247**, 368–378.
39 Y. M. Jia, J. W. Wang, K. Zhang, S. B. Liu, G. L. Chen, Y. F. Yang, C. M. Ding and P. Liu, Catalytic conversion of methanol to aromatics over nano-sized HZSM-5 zeolite modified by $ZnSiF_6 \cdot 6H_2O$, *Catal. Sci. Technol.*, 2017, **7**, 1776–1791.

